

# ORDER AND DISORDER PHENOMENA AT SURFACES OF BINARY ALLOYS

F. F. Haas

Institut für Physik, Johannes Gutenberg Universität Mainz, D 55099 Mainz

F. Schmid

Max-Planck Institut für Polymerforschung, Ackermannweg 10, D 55021 Mainz

[schmid@mpp-mainz.mpg.de](mailto:schmid@mpp-mainz.mpg.de)

K. Binder

Institut für Physik, Johannes Gutenberg Universität Mainz, D 55099 Mainz

[binder@chaplin.physik.uni-mainz.de](mailto:binder@chaplin.physik.uni-mainz.de)

**Abstract** We present recent Monte Carlo results on surfaces of bcc-structured binary alloys which undergo an order-disorder phase transformation in the bulk. In particular, we discuss surface order and surface induced disorder at the bulk transition between the ordered ( $DO_3$ ) phase and the disordered (A2) phase. An intricate interplay between different ordering and segregation phenomena leads to a complex surface behavior, which depends on the orientation of the surface under consideration.

The structure and composition of alloys at external surfaces and internal interfaces often differs significantly from that in the bulk. In most cases, this refers only to very few top layers at the surface, over a thickness of order 1 nm. In the vicinity of a bulk phase transition, however, the thickness of the altered surface region can grow to reach mesoscopic dimensions, of order 10–100 nm. If the bulk transition is second order, for example, the thickness of the surface region is controlled by the bulk correlation length, which diverges close to the critical point [1]. Close to first order bulk transitions, mesoscopic wetting layers may form [2].

While these various surface phenomena are fairly well understood in simple systems, such as surfaces of liquid mixtures against the wall of a container, the situation in alloys is complicated due to the interplay between the local structure, the order and the composition profiles. In alloys which undergo an order/disorder transition, for example, the surface segregation of one alloy component can induce surface order [3, 4, 5] or partial surface order [6, 7] at surfaces which are less symmetric than the bulk lattice with respect to the

ordered phase. Even more subtle effects can lead to surface order at fully symmetric surfaces[8, 9, 10, 11]. Furthermore, different types of order may be present in such alloys[12], which can interact in a way to affect the wetting behavior significantly [14, 15].

In this contribution, we discuss a situation where such an interplay of segregation and different types of ordering leads to a rather intriguing surface behavior: Surface induced disorder in a binary (AB) alloy on a body centered cubic (bcc) lattice close to the first order bulk transition between the ordered  $DO_3$  phase and the disordered bulk phase. Surface induced disorder is a wetting phenomenon, which can be observed when the bulk is ordered and the surface reduces the degree of ordering (usually due to the reduced number of interacting neighbors[13, 16, 17]). A disordered layer may then nucleate at the surface, which grows logarithmically as the bulk transition is approached. According to the theoretical picture, the surface behavior is driven by the depinning of the interface between the disordered surface layer and the ordered bulk.

In order to study the validity of this picture, we consider a very idealized minimal model of a bcc alloy with a  $DO_3$  phase: The alloy is mapped on an Ising model on the bcc lattice with negative nearest and next nearest neighbor interactions. The Hamiltonian of the system then reads

$$H = V \sum_{\langle ij \rangle} S_i S_j + V' \sum_{\langle\langle ij \rangle\rangle} S_i S_j - H \sum_i S_i; \quad (1)$$

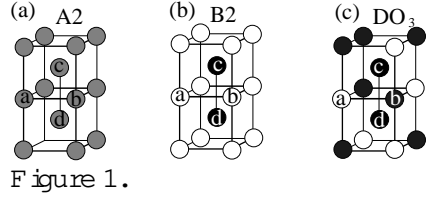
where Ising variables  $S = 1$  represent A atoms,  $S = -1$  B atoms, the sum  $\langle ij \rangle$  runs over nearest neighbor pairs,  $\langle\langle ij \rangle\rangle$  over next nearest neighbor pairs, and the field  $H$  is the appropriate combination of chemical potentials  $\mu_A$  and  $\mu_B$  driving the total concentration  $c$  of A in the alloy, ( $c = (\sum_i S_i + 1)/2$ ).

The phases exhibited by this model are shown in Figure 1. In the disordered (A2) phase, the A and B particles are distributed evenly among all lattice sites. In the ordered B2 and  $DO_3$  phases, they arrange themselves as to form a superlattice on the bcc lattice. The parameter  $\epsilon$  was chosen  $\epsilon = 0.457$ , such that the highest temperature at which a  $DO_3$  phase can still exist is roughly half the highest temperature of the B2 phase, like in the experimental case of FeAl. The resulting phase diagram is shown in Figure 2.

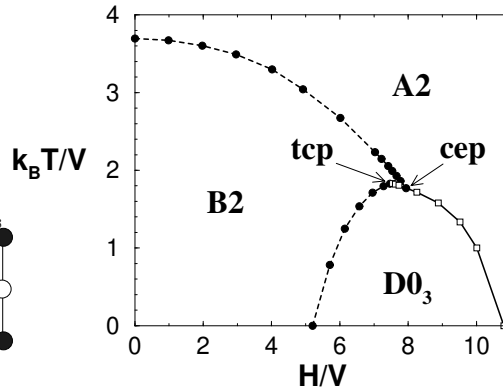
In order to characterize the ordered phases, it is useful to divide the bcc lattice into four face centered cubic (fcc) sublattices as indicated on Figure 1, and to define the order parameters

$$\begin{aligned} \sigma_1 &= (\sum_i S_{i_a} + \sum_i S_{i_b} - \sum_i S_{i_c} - \sum_i S_{i_d})/2 \\ \sigma_2 &= (\sum_i S_{i_a} - \sum_i S_{i_b} + \sum_i S_{i_c} - \sum_i S_{i_d})/2 \\ \sigma_3 &= (\sum_i S_{i_a} - \sum_i S_{i_b} - \sum_i S_{i_c} + \sum_i S_{i_d})/2; \end{aligned} \quad (2)$$

where  $\sum_i S_{i_\alpha}$  is the average spin on the sublattice  $\alpha$ . In the disordered phase, all sublattice compositions are equal and all order parameters vanish as a consequence. The B2 phase is characterized by  $\sigma_1 \neq 0$  and the  $DO_3$  phase by  $\sigma_1 \neq 0$  and  $\sigma_2 = \sigma_3 \neq 0$ . The two dimensional vector  $(\sigma_2; \sigma_3)$  is thus an



Ordered phases on the bcc lattice: (a) disordered A2 structure, (b) ordered B2 and (c) DO<sub>3</sub> structure. Also shown is assignment of sublattices a;b;c and d.



Phase diagram in the  $T-H$  plane. First order transitions are solid lines, second order transitions dashed lines. Arrows indicate positions of a critical end point (cep) and a tricritical point (tcp).

order parameter for DO<sub>3</sub> ordering, and the latter can be characterized conveniently in terms of its absolute value

$$\eta_{23} = \frac{\eta}{(\eta_2^2 + \eta_3^2)^{1/2}} = 2: \quad (3)$$

We have studied free (110) and (100) surfaces of this model at the temperature  $T = 1$   $k_B T = V$  in the DO<sub>3</sub> phase close to the transition to the disordered phase. To this end, we have first located the transition point very accurately by thermodynamic integration [18],  $H_0 = V = 10.00771$  [1]. We have then performed extensive Monte Carlo simulations of slabs each 100-200 layers thick, with free boundary conditions at the two confining (110) or (100) planes, and periodic boundary conditions in the remaining directions.

In all of our simulations, the average value of the Ising variable in the top layer was one, i.e., the top layer was completely filled with A atoms. Having stated this, we shall disregard this layer in the following and discuss the structure starting from the next layer underneath the surface. The layer order parameters  $\eta_i(n)$  and the layer compositions  $c(n)$  can be determined in a straightforward manner for (110) layers, since they contain sites from all sublattices. In the case of the (100) layers, it is useful to define  $\eta_i$  based on the sublattice occupancies on two subsequent layers.

Fig. 3 shows the calculated profiles for two choices of  $H$  close to the transition. One clearly observes the formation of a disordered film at the surface, which increases in thickness as the transition point is approached. The film is characterized by low order parameters  $\eta_1$  and  $\eta_{23}$ , and by a slightly increased concentration  $c$  of A sites. The structure very close to the surface depends

on its orientation: The composition profiles display some characteristic oscillations at a (110) surface, and grow monotonously at a (100) surface. The order  $\psi_{23}$  drops to zero. The order  $\psi_1$  drops to zero at the (110) surface, and at the (100) surface, it changes sign and increases again in the outmost two layers. The latter is precisely an example of the segregation induced ordering mentioned earlier [3, 4, 5].

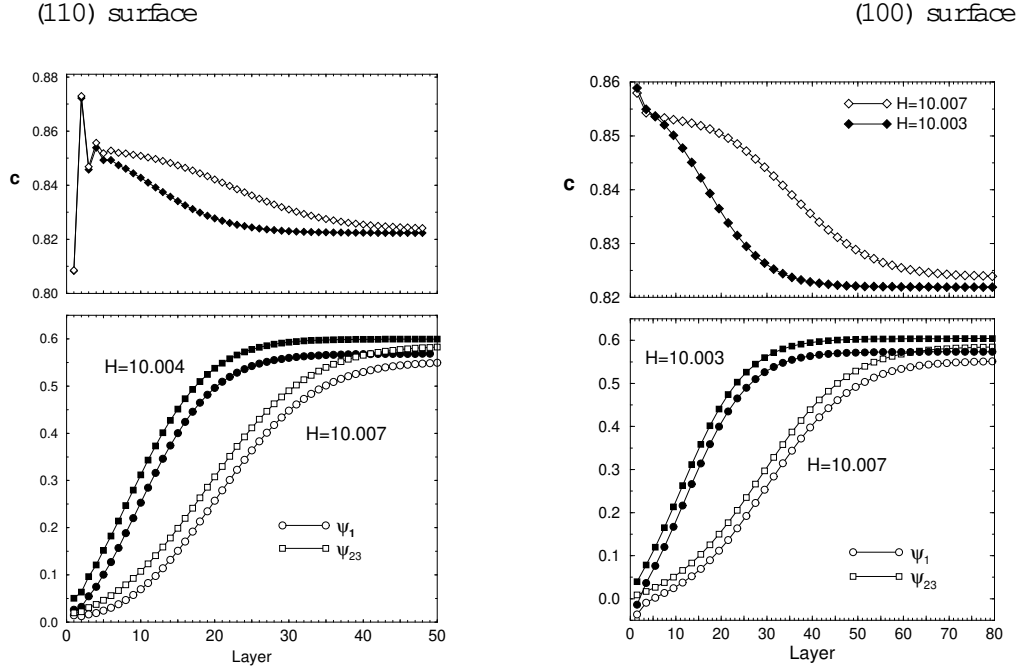


Figure 3.

Profiles of the total concentration (top) and order parameters  $\psi_1$  (bottom, circles) and  $\psi_{23}$  (bottom, squares) at the (110) surface (left) and at the (100) surface (right) for different fields  $H$  in units of  $V$  as indicated.

We can thus distinguish between two interesting regions in these profiles: The near-surface region, where the properties of the profiles still reflect the peculiarities of the surface, and the interfacial region, where the profiles are determined from the properties of the interface separating the disordered surface film from the ordered bulk.

The structure of the profiles in the interfacial region is basically determined by the fluctuations of the interface, which are characterized by a transverse correlation length  $\xi_k$ . The latter is in turn driven by the thickness of the film and the interfacial tension or, more precisely, by a rescaled dimensionless interfacial tension

$$1/\xi_k^2 = 4/\xi_b^2 - \beta k_B T; \quad (4)$$

with the bulk correlation length  $\xi_b$ . The renormalization group theory of critical wetting [2], which should apply here [16], predicts that the transverse

correlation length diverges according to a power law

$$\xi_k / \xi_{k=1} = (H_0 - H)^{-\nu_k} \quad (5)$$

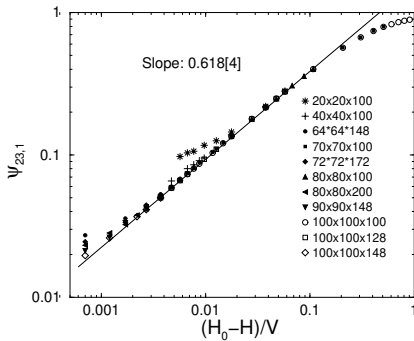
as  $H_0$  is approached, with the exponent  $\nu_k = 1/2$ . With this knowledge, one can calculate the effective width of the order parameter profiles,  $\xi_k / \xi_{k=1} \ln(H_0 - H)$ , the profiles of layer susceptibilities etc. We have examined these carefully at the (110) interface and the (100) interface, both for the order parameters  $\psi_1$  and  $\psi_{23}$ , and we could fit everything nicely into the theoretical picture. Our further discussion here shall focus on the near-surface region.

Assuming that the order in the near-surface region is still determined by the fluctuations of the interface, the theory of critical wetting predicts a power law behavior

$$\psi_{23,1} / (H_0 - H)^{\nu_1} \quad (6)$$

for value  $\nu_1$  of the order parameter directly at the surface, regardless of the structure of the surface. Figure 4 shows that, indeed, the surface order parameter  $\psi_{23,1}$  decays according to a power law at both the (110) and the (100) surface, with the same exponent and the exponent is in both cases identical within the error,  $\nu_1 = 0.618$ . Furthermore, we notice strong finite size effects close to the  $H_0$ . Since these are asymptotically driven by the ratio  $(L = \xi_k)$ , they can be exploited to determine the behavior of  $\xi_k$  as the phase transition is approached, i.e., the exponent  $\nu_k$ . The finite size scaling analysis yields  $\nu_k = 1/2$  [19], in agreement with the theory.

(110) surface



(100) surface

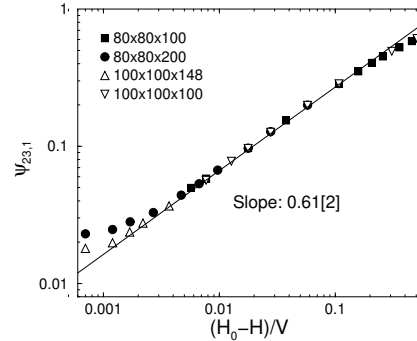


Figure 4.

Order parameter  $\psi_{23}$  at the surface at the (110) surface (left) and the (100) surface (right) vs.  $(H_0 - H)/V$  for different system sizes  $L \times L \times D$  as indicated. Solid line shows power law with exponent  $\nu_1 = 0.618$ .

The profiles of  $\psi_{23}$  thus seem entirely determined by the depinning of the interface, in agreement with the standard theory of critical wetting. The situation is however different when one looks at the other order parameter,  $\psi_1$ . This is not particularly surprising in the case of the (100) surface. We

have already noted that this surface breaks the symmetry with respect to the  $\phi_1$  ordering, hence the segregation of A particles to the top layer induces additional  $\phi_1$  order at the surface (Figure 5). The (110) surface, on the other hand, is not symmetry breaking. The order  $\phi_1$  decays at the surface, yet with an exponent  $\phi_1 = 0.801$  which differs from that observed for  $\phi_{23}$  (Figure 6). Even more unexpected, the finite size effects cannot be analyzed consistently with the assumption that the transverse correlation length diverges with the exponent  $\phi_k = 1/2$ , but rather suggest  $\phi_k = 0.7 - 0.05$ . The order parameter fluctuations of  $\phi_1$  at the surface seem to be driven by a length scale which diverges at  $H_0$  with an exponent different from that given by the capillary wave fluctuations of the depinning interface.

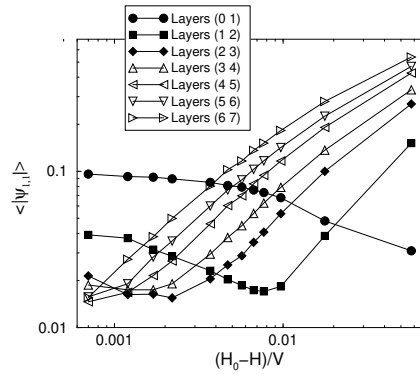


Figure 5.  
Order parameter  $\phi_1$  in the first layers underneath the (100) surface vs.  $(H_0 - H)/V$ .

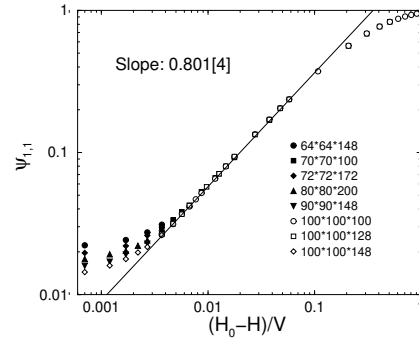


Figure 6.  
Order parameter  $\phi_1$  at the (110) surface vs.  $(H_0 - H)/V$  for different system sizes  $L \times L \times D$  as indicated. Solid line shows power law with exponent  $\phi_1 = 0.801$ .

To summarize, we have seen that the phenomenology of surface induced disorder in a relatively simple bcc alloy with just two coupled types of ordering is much more complex than predicted by the standard theory of surface induced disorder and critical wetting. Looking at our profiles, we were able to distinguish between two regions, the near-surface region and the interfacial regions. In the situations studied in our simulations, it seemed that these regions could be well separated from each other. Some rapid variations of the profiles in the near-surface region, are followed by smooth changes in the interfacial region. The local surface structure affects the total composition profile relatively strongly, and has practically no influence on the profile of the  $\phi_{23}$  order. In the case of the B2 order,  $\phi_1$ , the situation is more intriguing. The symmetry breaking (100) surface induces local order in the near-surface region which apparently does not couple to the interface. At the non-symmetry breaking (110) surface,  $\phi_1$  was found to exhibit qualitatively new and unexpected power law behavior as the wetting transition is approached.

The last observation clearly requires further exploration in the future. The picture will be even more complex in situations where the near-surface profiles

and the interfacial profiles cannot be separated any more. We expect that this could be the case, e.g., at (111) surfaces, which break the symmetry with respect to both B2 and DO<sub>3</sub> ordering.

F.F. Haas was supported by the Graduiertenförderung of the Land Rheinland-Pfalz.

## References

- [1] For reviews on surface critical phenomena see K. Binder in Phase Transitions and Critical Phenomena, Vol. 8, p. 1 (1983), C. Domb and J.L. Lebowitz eds., Academic Press, London; S.Diehl, *ibid*, Vol. 10, p.1. (1986).
- [2] For reviews on wetting see, e.g., P.G. de Gennes, Rev. Mod. Phys. 57, 827 (1985); S.Dietrich in Phase Transitions and Critical Phenomena, C. Domb and J.L. Lebowitz eds (Academic Press, New York, 1988), Vol. 12; M. Schick in Les Houches, Session XLV III { Liquids at Interfaces, J. Charvolin, J.F. Joanny, and J. Zinn-Justin eds (Elsevier Science Publishers B.V., 1990).
- [3] F. Schmid, Zeitschr. f. Phys. B 91, 77 (1993).
- [4] S. Krimmel, W. Donner, B. Nickel, and H. Dosch, Phys. Rev. Lett. 78, 3880 (1997).
- [5] A. Drewitz, R. Leidl, T.W. Burkhardt, and H.W. Diehl, Phys. Rev. Lett. 78, 1090 (1997); R. Leidl and H.W. Diehl, Phys. Rev. B 57, 1908 (1998); R. Leidl, A. Drewitz, and H.W. Diehl, Int. Journal of Thermophysics 19, 1219 (1998).
- [6] H. Reichert, P.J. Eng, H. Dosch, I.K. Robinson, Phys. Rev. Lett. 74, 2006 (1995).
- [7] F. Schmid, in Stability of Materials, p. 173, A. Gonis et al eds., (Plenum Press, New York, 1996).
- [8] L. Mailander, H. Dosch, J. Peisl, R.L. Johnson, Phys. Rev. Lett. 64, 2527 (1990).
- [9] W. Schweika, K. Binder, and D.P. Landau, Phys. Rev. Lett. 65, 3321 (1990).
- [10] W. Schweika, D.P. Landau, and K. Binder, Phys. Rev. B 53, 8937 (1996).
- [11] W. Schweika, D.P. Landau, in Computer Simulation Studies in Condensed-Matter Physics X, P. 186 (1997).
- [12] for reviews see D. De Fontaine in Solid State Physics 34, p. 73 H. Ehrenreich, F. Seitz and D. Tumbell eds., Academic Press, New York 1979; K. Binder in Festkörperprobleme (Advances in Solid State Physics) 26, p. 133, P. Grosse ed., Vieweg, Braunschweig 1986.
- [13] R. Lipowsky, J. Appl. Phys. 55, 2485 (1984).
- [14] E.H. Hauge, Phys. Rev. B 33, 3323 (1985).
- [15] D.M. Kroll, G. Gompper, Phys. Rev. B 36, 7078 (1987); G. Gompper, D.M. Kroll, Phys. Rev. B 38, 459 (1988).
- [16] D.M. Kroll and R. Lipowsky, Phys. Rev. B 28, 6435 (1983).
- [17] H. Dosch, Critical Phenomena at Surfaces and Interfaces (Evanescent X-ray and Neutron Scattering), Springer Tracts in Modern Physics Vol 126 (Springer, Berlin, 1992).
- [18] K. Binder, Z. Phys. B 45, 61 (1981).
- [19] F.F. Haas, Dissertation Universität Mainz (1998); F.F. Haas, F. Schmid, and K. Binder, in preparation.